

# Intensive electron emission in a strong electric field in vacuum nanoelectronics and high-power electronics

G.N. Fursey\*

*Surface Physics and Electronics Research Centre, Bonch-Bruевич State University of Telecommunications, St Petersburg, Russia*

This paper briefly discusses the remarkable characteristics of the processes of field electron (FE) and explosive electron (EE) emission in a strong electric field. Special emphasis is placed on the recently discovered extraordinary fundamental effects occurring at carbon nanoclusters: the low-threshold FE and EE. Important possible practical applications of these phenomena are considered, including the opportunity to develop a new type of very compact X-ray devices.

**Keywords:** explosive emission, field emission, graphene, high-current electronics, low threshold field emission, nanotubes, portable X-ray devices, vacuum nanoelectronics

## 1. Introduction

Emission processes occur in strong electric fields; their intensity exceeds by millions of times the intensity of all other emission types, such as thermal emission, photoemission, secondary emission, etc. This provides unique opportunities for their practical employment in different technical areas, including two very important ones: vacuum nanoelectronics and high-current electronics [1–3]. This paper deals with an analysis of these processes, with their quantitative description, and with their peculiarities.

*Field emission* (FE) is initiated at a field strength of  $3 \times 10^7$ – $10^8$  V/cm. This process is conditioned by electron tunnelling from the condensed phase into the vacuum (cf. ref. 1).

A new emission process has been discovered at an extremely high field strength of  $> 10^8$  V/cm, occurring with an explosion-like change of phase of a condensed matter (solid or liquid) into a dense nonequilibrium plasma. This type of emission has been named *explosive electron emission* (EE) [4, 5] (cf. also refs 3 and 6).

Such emission is generated in nanometre-sized areas of the cathode surface with extremely high emission current densities passing through them.

---

\* E-mail: g.fursey@gmail.com

The unique and peculiar characteristics of emission processes in a strong electric field from carbon nanoclusters: nanotubes and graphenes have been discovered during the last few years. It was shown in direct experiments [7–9] (cf. also ref. 1, §8.13) that the threshold fields of the emission process excitation are 100–1000 times lower for these materials than for metals or semiconductors, amounting to a mere  $10^5$ – $10^6$  V/cm. This extraordinary lowering provides unique opportunities for practical applications of FE and EE in vacuum nanoelectronics and high-current electronics. In particular, one may think of designing low-voltage, multi-emitter arrays for field emission displays, microwave devices and other vacuum nanoelectronic devices, as well as for a number of types of high-current devices; e.g., one might make very compact pulsed X-ray devices.

In this paper we consider a number of newly discovered features of the emission processes in strong electric field as well as new application opportunities.

## 2. Field electron emission from metals

The field emission process is a unique type of electron emission; it is due exclusively to quantum-mechanical effects—tunnelling of electrons into the vacuum. In metals and semiconductors this phenomenon occurs at high electric fields ( $3 \times 10^7$  V/cm). An adequate quantitative description of the process is given by the Fowler–Nordheim theory [13]. The field emission current density at  $T = 0$  follows the classic Fowler–Nordheim formula

$$j = \frac{e^3}{8\pi h} \frac{F^2}{t^2(y)\varphi} \exp\left[-6.83 \times 10^7 \frac{\Phi^{3/2}}{F} \vartheta(y)\right], \quad (1)$$

where  $\varphi$  is the work function. Substituting the values of constants and expressing  $\varphi$  in eV,  $F$  in V/cm and  $j$  in  $\text{A}/\text{cm}^2$  we have,

$$j = 1.54 \cdot 10^{-6} \frac{F^2}{t^2(y)\varphi} \exp\left[-6.83 \times 10^7 \frac{\Phi^{3/2}}{F} \vartheta(y)\right], \quad (2)$$

where  $y = 3.79 \times 10^{-4} \times \sqrt{F}/\varphi$  and  $t(y) = \vartheta(y) - (2y/3)(d\vartheta(y)/dy)$ ;  $\vartheta(y)$  and  $t(y)$  have been tabulated [10] and can be found in a number of works (cf. ref. 1, §1.1, p. 3);  $t(y)$  is the pre-exponential factor, which is close to unity and varies weakly with the argument. In many cases it is justifiably set to unity. The Nordheim function  $\vartheta(y)$  varies significantly with  $y$  and, correspondingly, so does  $F$ .

Formulae (1) and (2) give an excellent description of the experimentally observed exponential dependence of the emission current on field strength  $F$  and work function  $\varphi$ . In the so-called Fowler–Nordheim coordinates the functional dependence  $\ln j = f(1/F)$  or, correspondingly,  $\ln I = f(1/U)$  is a straight line over a wide range of emission current values. Here,  $I = j \times S$  is the emission current, with  $S$  as the emitting area, and  $F = \beta U$ , where  $\beta$  is a geometric quotient determined by the geometry of the vacuum gap.

## 3. Maximum current densities of field emission

### 3.1 Theoretical limit of FE

One of the most remarkable results of field emission quantum theory is the prediction of very high emission current densities. They are possibly due to two factors: (1) no energy is required

for maintaining the emission process if electrons leave the solid by a tunnelling mechanism; that is, the emitter does not need to be heated, irradiated or otherwise excited by some external energy source; and (2) there is a very large reservoir of electrons near the Fermi level of a metal.

As the density of the conduction band electrons in metals is of the order of  $10^{22}$  to  $10^{23}$   $\text{cm}^{-3}$ , it can be assumed that the electrons in the metal flowing towards the metal/vacuum interface can sustain a current density of about  $10^{11}$   $\text{A/cm}^2$  (cf. ref. 1, pp. 31–32):

$$j = \frac{\pi e m_e E_F^2}{h^3} \cong 4.3 \cdot 10^9 E_F^2 \approx 10^{11} \text{ A/cm}^2 \tag{3}$$

where  $E_F$  is the Fermi energy (in eV) measured from the bottom of the conduction band.

Actually, the field emission current density is usually lower than predicted by theory due to the initiation of a vacuum arc due to the onset of field emission instability at high current densities. When an arc is induced, the cathode begins to melt and ceases to be a controllable field emission cathode.

It has been demonstrated in experiments that the maximum current densities for refractory metals (W, Re, Ta, Mo etc.) and refractory compounds ( $\text{LaB}_6$ , ZrC) may reach steady-state values of up to  $10^7$   $\text{A/cm}^2$ , up to  $10^8$   $\text{A/cm}^2$  in microsecond pulses, and up to  $10^9$   $\text{A/cm}^2$  in nanosecond pulses. The highest field emission current densities achieved experimentally are given in Table 1 (cf. ref. 1, §3.5, p. 50).

Table 1. Highest field emission current densities achieved experimentally.

Material	$T / \text{s}$	$j_{\text{max}} / \text{A cm}^{-2}$	Authors
W	$10^{-6}$	$10^8$	Dyke et al. (1953, 1960)
	DC mode	$10^7$	
	$10\text{--}10^{-3}$	$2 \times 10^7$	Fursey, Kartsev (1970)
Mo	$10^{-3}$	$8 \times 10^6$	Fursey, Krotevich et al. (1984, 1985)
Nb		$3 \times 10^6$	
$\text{LaB}_6$ ZrC	$3 \times 10^{-6}$	$10^7\text{--}10^8$	Elinson et al. (1954, 1964)
Ta	$4 \times 10^{-6}$	$5 \times 10^7$	Fursey et al. (1963, 1964)
Re		$(3\text{--}5) \times 10^7$	
W	$10^{-7}$	$3 \times 10^8$	Mesyats, Fursey et al. (1969, 1970)
	$10^{-8}$	$(5\text{--}6) \times 10^8$	
	$10^{-9}$	$10^9$	

### 3.2 *Extremely high current density FE*

Higher current densities approaching the theoretical limit were obtained by special techniques: at very short voltage pulse lengths (nanoseconds), at a very cold cathode surface (temperatures as low as 4.2 K), and at emission take-off from purposely produced nanometre-sized areas of the cathode surface: see Table 2 (cf. ref. 1, §3.5, p. 56).

Table 2. Extremely high current density FE.

Conditions	Material	Record current densities / $\text{A cm}^{-2}$	Authors
Nanosecond duration ( $\tau_{\text{pulse}} = 5 \text{ ns}$ , $T = 300 \text{ K}$ )	W	$10^9$	Mesyats, Fursey et al. (1969, 1970)
Deep cooling ( $\tau_{\text{pulse}} = 10 \text{ ns}$ , $T = 4.2 \text{ K}$ )	W	$10^9$	Fursey et al. (1979)
Small emission spot (spot diameter $d \approx 100 \text{ \AA}$ , $\tau_{\text{pulse}} = 4 \text{ ms}$ , $T = 300 \text{ K}$ )	W+Zr	$5 \times 10^9$	Fursey, Shakirova (1966)
Supersmall emission spot ( $d = 20\text{--}30 \text{ \AA}$ , dc mode, $T = 300 \text{ K}$ )	W+Zr	$10^9$	Fursey, Glazanov et al. (1995)
Nanotips (dc mode, $T = 300 \text{ K}$ )	W	$10^9\text{--}10^{10}$	Shrednik et al. (1975)
Supersmall nanotips (emitter radius $r_{\text{em}} = 10\text{--}20 \text{ \AA}$ , $\tau_{\text{pulse}} = 100 \text{ ms}$ , $T = 300 \text{ K}$ )	W	$10^{10}\text{--}10^{11}$	Fursey, Glazanov et al. (1998)

#### 4. Field emission from carbon nanoclusters: exceptionally low threshold of field emission from nanotubes and graphene

Carbon has proved to be a very special material, very much distinct from metals or semiconductors, which manifests itself particularly in novel carbon structures such as nanotubes and graphene.

The work function for carbon in the form of graphite is known to be in the same range as that for metals; correspondingly, FE current is initiated at a field strength of the order of  $3 \times 10^7 \text{ V/cm}$ . We managed to show experimentally that the threshold of field emission excitation for nanotubes and graphene is 2–3 orders of magnitude lower than what was experimentally observed before for solids, for the “traditional” case of metals and semiconductors [1, 2, 7–9]. This phenomenon was named “low-threshold emission”. The threshold field strengths of the excitation of FE are compared in Table 3.

Table 3. Threshold field strengths /  $\text{V cm}^{-1}$ .

“Traditional” excitation threshold, $F_0$ at $\phi = 4.5\text{--}5 \text{ eV}$	$\approx (3\text{--}5) \times 10^7$
Threshold field for vacuum gap macrogeometry, $F_{\text{macro}}$	$\approx 10^4$
Threshold field with maximum possible cathode surface roughness ( $\beta = 10$ ) $F_{\text{micro}}$	$\approx 10^5$

Note:  $\phi$  is the cathode surface work function,  $\beta = F/U$  is a geometrical factor, and  $U$  is the anode–cathode voltage.

An explanation of the low-threshold emission mechanism was obtained by means of field electron microscopy and high-resolution transmission and scanning electron microscopies.

The layout of FE experiments is presented in Fig. 1. Current–voltage characteristic of FE in the Fowler–Nordheim coordinates were analysed, field emission microscopy images were studied in detail, and a correlation was meticulously looked for between the field emission behaviour and the electron microscopy images in the scanning microscope.

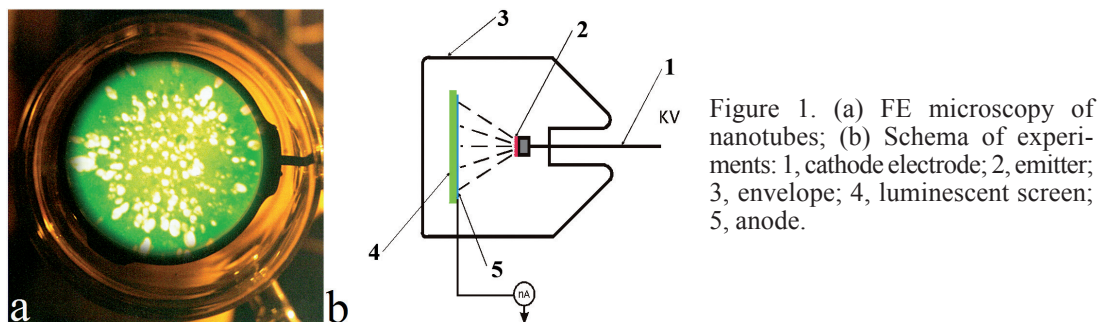


Figure 1. (a) FE microscopy of nanotubes; (b) Schema of experiments: 1, cathode electrode; 2, emitter; 3, envelope; 4, luminescent screen; 5, anode.

#### 4.1 Nanotubes

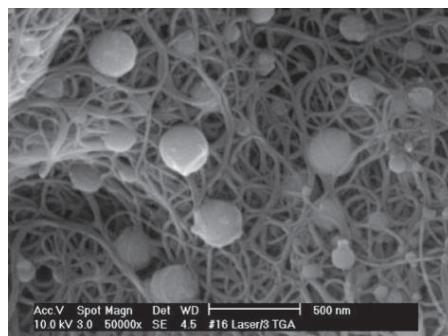
The present work is devoted to the investigation of carbon nanotubes formed in plasma by electric arc evaporation of graphite [12]. The carbon nanotubes were formed during helium arc discharge vaporization of graphite directly on the cathode. The final products of the conversion of carbon atoms evaporated from the anode represented a “cathode deposit” containing carbon nanotubes.

Classical field emission microscopy and high resolution scanning electron microscopy were employed to study the emitting surface. The morphology of the “cathode deposit” surface was studied in a Cam Scan scanning electron microscope (resolution 20 Å).

The results from experiments with the nanotubes are illustrated in Figs 1, 2 and 3. A base in the form of a cylindrical rod of 3–5 mm diameter having the carbon deposit containing nanotubes lying on its surface was used as the cathode. FE images show a fairly even distribution of emitting centres over the cathode surface (Fig. 1a).

An important new fact observed is that the low field emission threshold is virtually insensitive to the nanotube orientation relative to the surface. The “low-threshold emission” is observed when the nanotubes are sticking out perpendicular to the surface and when they are lying down flat upon it (Fig. 2).

Figure 2. Scanning electron micrograph of the carbon nanotubes (for details see text).



The FE current–voltage characteristics for all the specimens studied were straight lines in the Fowler–Nordheim coordinates (Fig. 3).

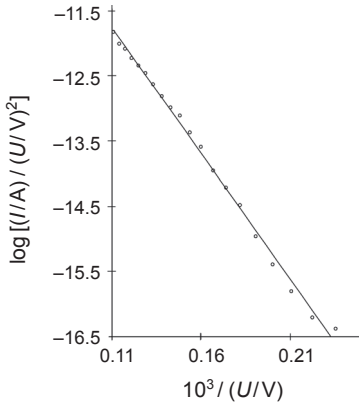


Figure 3. FE current–voltage characteristic of the nanotubes.

#### 4.2 Graphene

Graphene arrays were produced by means of detonation synthesis [11], forming scale-like structures having typical dimensions of 0.3 mm. These scales were set onto a metallic substrate and fixed on it with a binder: aquadag or silver paste (Figs 4 and 5).

Figure 4. Schematic image of the cathode: (1) coating of carbon nanoclusters; (2) binder; and (3) base.

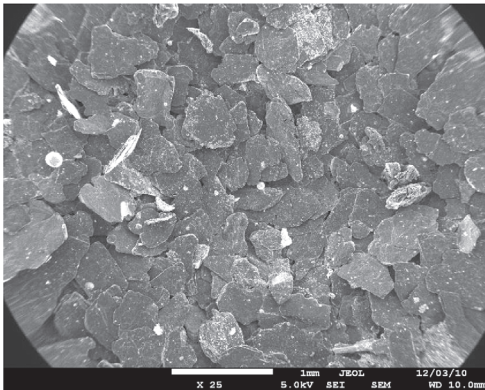
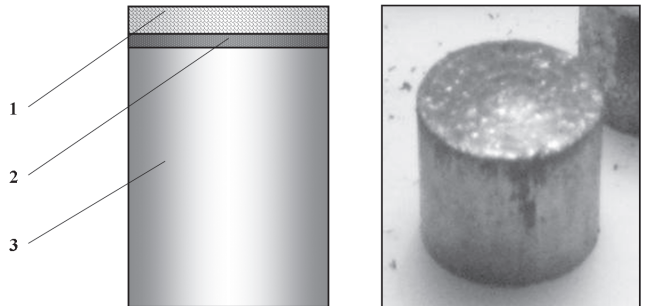


Figure 5. Scanning electron micrograph of a cathode surface covered by graphene flakes.

Experiments were conducted in a special vacuum chamber (Fig. 6), in which the cathode (1)–anode (3) distance could be controllably varied. The field-emission current was detected with collector 6. The chamber was equipped with a field emission microscopy attachment. Field emission images were displayed on fluorescent screen 8. A general view of the vacuum chamber is shown in Fig. 6a.

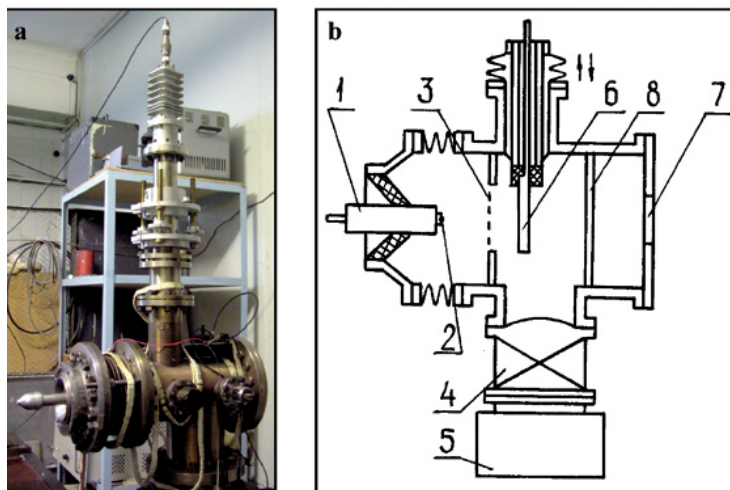


Figure 6. General view (a) and construction (b) of the experimental chamber. (b): 1, high-voltage lead; 2, emitter; 3, anode grid; 4, vacuum pump; 5, sorption pump; 6, electron collector; 7, window for photography; 8, fluorescent screen.

The high voltage could be varied in the interval 0–15 kV. The voltage was applied to the cathode (1), and the current was measured with a nanoammeter connected to the collector plate (6). The experimental volume was evacuated using magnetodischarge pump 4 down to a residual pressure of  $10^{-8}$ – $10^{-7}$  Torr.

Shown in Fig. 7 are FEM images of the graphene scale cathode. One can see distinctly the images of individual scales. Fig. 7a shows a corresponding SEM image of the cathode surface, and in Fig. 8 several cathode surface fragments are presented with a greater magnification. One can see that the surface does actually have a graphene-like pattern. One can assume that the surface of the scales, being rather smooth, yields a field strength magnification coefficient  $< 10$ . FE current–voltage characteristics for the graphene structures are linear in the Fowler–Nordheim coordinates, very much like for the nanotubes.

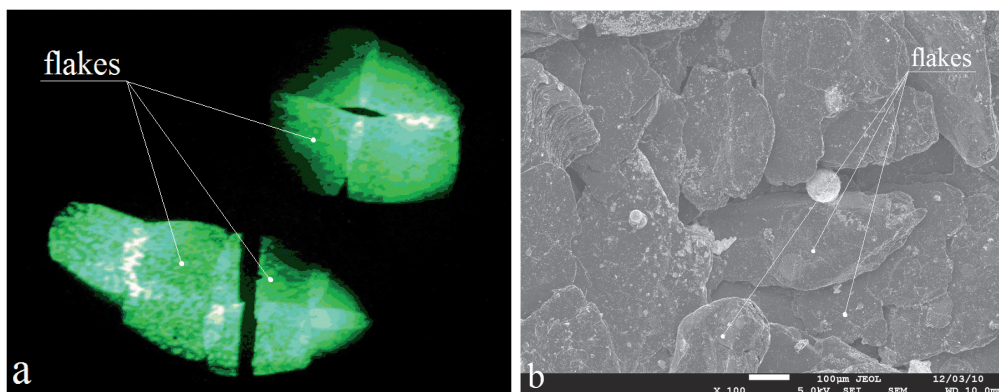


Figure 7. (a) field emission picture from graphene-like clusters; (b) scanning electron micrograph showing the structure of the cathode surface.

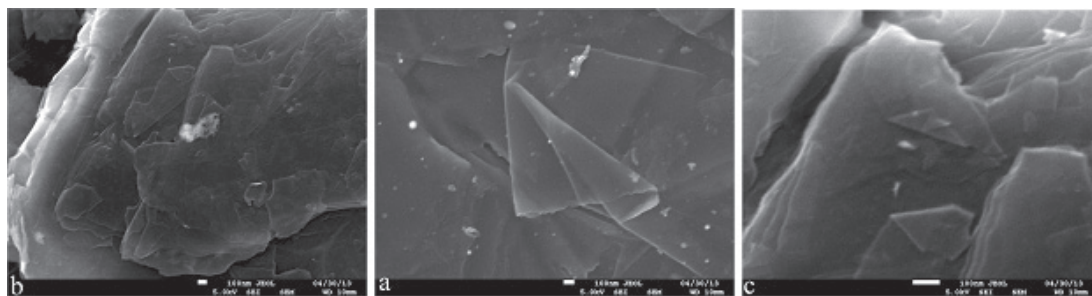


Figure 8. Local fragments of different parts of the cathode surface.

One should emphasize, however, that this resemblance to the Fowler–Nordheim law is a mere coincidence in both cases (graphene and nanotubes). Analysis of current–voltage characteristics shows that Fowler–Nordheim theory is not applicable here. An attempt was made to compute the work function from current–voltage slopes [7, 8], but even if we deliberately overestimate the field magnification coefficient, taking it equal to 10, or even to 100, we obtain unreasonably low values of  $\phi = 10^{-2}$ – $10^{-1}$  eV, to which it is difficult to ascribe physical meaning. Hence one can assume that the Fowler–Nordheim theory is incapable of an adequate description of low-threshold field electron emission (FEE). The idea of ascribing the phenomenon of low-threshold FEE to quantum dimensional effects has been consistently developed in refs 7–9.

### 4.3 Interpretation of low-threshold phenomena

At present there is no clear interpretation of the extremely low threshold field for the electron emission from carbon nanoclusters.

The author and his colleagues Pavlov and Yafyasov [7–9, 14] have suggested a possible mechanism of this effect, based on the idea of dimensional quantizing.

As noted in the Introduction, the threshold field needed to initiate field emission from carbon nanoclusters had been shown to be several orders of magnitude (100–1000 times) lower than for normal metals and semiconductors.

A few attempts were made to explain this effect by field enhancement on microprotrusions on the cathode surface [15]. We propose a different explanation, the gist of which is resonance tunnelling of electrons through a potential barrier. We have staged the experiments described above to refute the trivial idea of local field enhancement. The absence of irregularities that might cause a more than tenfold field enhancement at the emitting surface is direct evidence for an insignificant role of microprotrusions in this phenomenon. A detailed electron microscopic examination of the emitting surface covered by detonation-produced particles shows that the surface contains graphene. That is distinctly seen in the micrographs presented in Fig. 8. The surface is smooth, with no visible signs of unevenness. The linear shape of the  $I$ – $V$  characteristics in the Fowler–Nordheim coordinates suggests that emission is governed by tunnelling. Nevertheless, if one tries to derive the work functions from the slope of the  $I$ – $V$  characteristic, one obtains unreasonably low values, in the range of 0.01–0.10 eV, which have no underlying physical mechanism.

We have, therefore, proposed a different mechanism [7–9], based on resonance properties of the potential barrier at the carbon cluster–vacuum interface. The point is that quantization-induced discrete resonance levels emerge in the energy band structure of the space-charge region near the emitter surface when the electric field is applied. That makes the potential barrier much more transparent for electrons possessing certain discrete energies.

We have suggested a description of the field emission from carbon structures in terms of size quantization, taking account of the 2D structure of the carbon cathode surface, and the observed low-threshold field emission from the carbon nanoclusters is explained by resonance electron tunnelling into the vacuum [7–9].

### **5. Explosive emission (EE) phenomena—stages of the EE process**

When the field emission current reaches its maximum, the emitter (a tip, or microprotrusions on the cathode surface) is irrevocably destroyed. In practical terms, that means complete destruction of the field emission cathode. The destruction occurs in an explosion-like manner, taking a time ( $10^{-9}$ – $10^{-10}$  s) orders of magnitude smaller than all the preceding processes. The explosion-like character is due to a sharply nonlinear energy evolution in the emitter.

The process is basically similar to the so-called nonlinear processes with acceleration (blow-up processes) [16], due to the sharp change of all the thermal characteristics of matter in a pre-explosion state.

A change of phase, “condensed matter to dense plasma”, occurs at the moment of the local explosion, and at that very moment an intense emission of electrons takes place, with an emission current orders of magnitude larger than the current of the preceding FE.

The remarkable feature of the phenomenon, the discovery of which was reported in ref. 4 (cf. ref. 2), is the spread of the process over a substantial portion of the cathode surface rather than its confinement to a single initial explosion site.

It was shown experimentally that the liquid phase is always generated in the explosion area (cf. ref. 17). The liquid is unstable in the strong electric field and nanocapillary waves are formed on its surface, whose crests actually act as new emission centres. At the end of the pulse these nanowaves are frozen at the surface to become geometrical nanostructures providing the means to initiate a new cycle of explosive emission when applying a new pulse. This phenomenon was named “explosive electron emission” (EE) [4, 5] (cf. ref. 6), in accordance with the emission excitation mechanism. Thus, one can divide the whole process of EE development into 4 main stages:

- (1) Explosion of a nanotip followed by phase change development and electron current peak;
- (2) Propagation of the process over the cathode surface;
- (3) Formation of the liquid phase and generation of microprotrusions in the form of nanometre-sized waves on the liquid surface;
- (4) Solidification (freezing) of the microprotrusions resulting in the formation of a nanogeometry to enable the initiation of a new EE cycle.

EE initiation by FE at an explosion of a solitary nanotip is demonstrated by the oscillogram—curve 6 in Fig. 9. The dynamics of EE development are presented in Fig. 10.

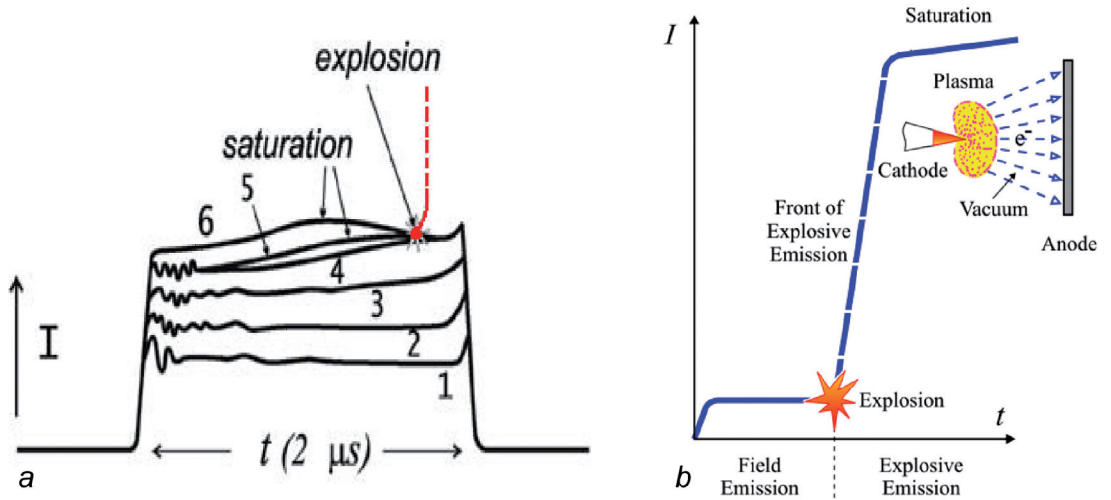


Figure 9. (a) current oscillograms of the pre-explosive stage (1–6: current versus time traces for different values of pulse voltage  $U_n > U_m$  for  $n > m$ ) [4]; (b) diagram of explosive emission excitation.

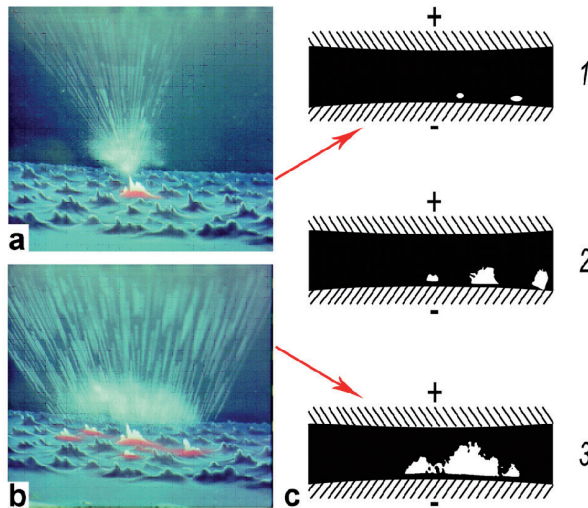


Figure 10. (a, b) visualization of explosive electron emission: drawn “animation” picture of the development [4]; (c) sequence of frames from Mesyats’ experiments [5].

Thus, explosive electron emission is a distinct phenomenon occurring after the explosion of a field electron emitter caused by an extremely high field emission current density. Under such conditions, a quasisteady-state phase change of the condensed matter of the cathode into dense plasma takes place, accompanied by emission into the vacuum of an intense flow of electrons. After initiation of the events of local EE, the process rapidly expands over the cathode surface as a result of the spread of the plasma, thus sustaining the emission process by involving in it further areas of the surface. The models described in ref. 4 were verified in studies by Mesyats et al. [5] (cf. Figs 10a and 10b).

It is established by now that the characteristic time of EE initiation is  $10^{-9}$ – $10^{-10}$  s, EE current density may be up to  $10^8$  A/cm<sup>2</sup> and greater, the velocity of plasma propagation in the vacuum gap is on the order of  $2$ – $3 \times 10^6$  cm/s, and the density of the nonequilibrium plasma may be as large as  $10^{20}$  cm<sup>-3</sup> (see refs 3, 6).

### **5.1 Explosion emission from carbon materials**

One of the main requirements for EE stability and recurrence is the reproducibility of cathode microgeometry after each initiation (i.e., after each emission pulse). In this regard, carbon exhibits two remarkable features, which will be described in the following two sections.

### **5.2 Formation of nanoprotuberances on the carbon**

Under normal pressure conditions the carbon bypasses the liquid state and sublimates (carbon passes into the liquid state only under high pressure conditions—more than  $10^2$  atmospheres). However, it has been noticed that in explosive emission the surface of the carbon melts in the areas near the explosion centres. This predetermines the special conditions for microrelief preservation by EE impulse termination. Freezing and solidification of the nanometre waves, in the case of carbon, occurs now not at the cost of temperature pull-down in the locally imploded areas of the cathode but due to pressure relief by plasma spread. Since this pressure relief occurs much faster than cooling down, it enables the microasperity on the surface to be preserved and enhances the reproducibility of the explosive emission current impulses from activation to activation. In addition, the forming of the small protuberances allows a decreased voltage for EE initiation.

It has been established that the surface layer of the carbon emitter is liquefied during an explosive electron emission (EE) pulse to form very fine (on the scale of nanometres) tips with curvature radii  $r < 10$  nm. Such tips are evenly distributed over the carbon emitter surface with a density of the order of  $10^8$  cm<sup>-2</sup>. The liquid phase appearance and the nanoprotuberances forming on the surface of the carbon are shown in Figures 11 and 12.

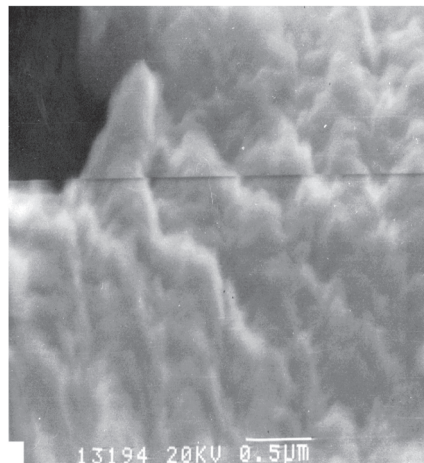
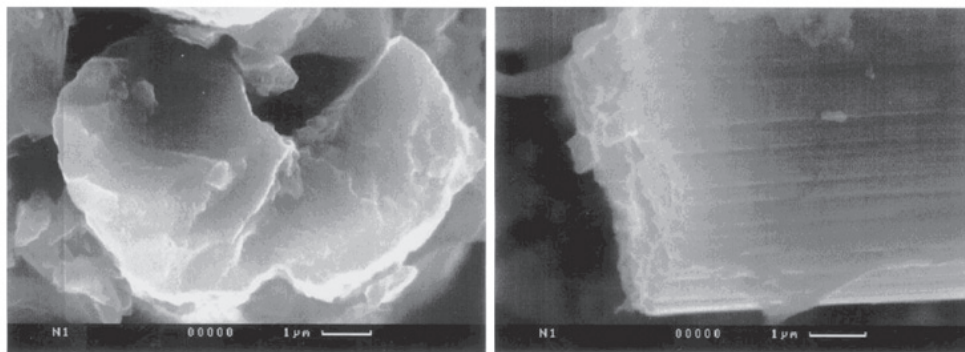


Figure 11. Frozen trace of the nanocapillary waves forming at the carbon surface by EE.

### Initial state of carbon surface



### Nanotip formation from liquid carbon phase

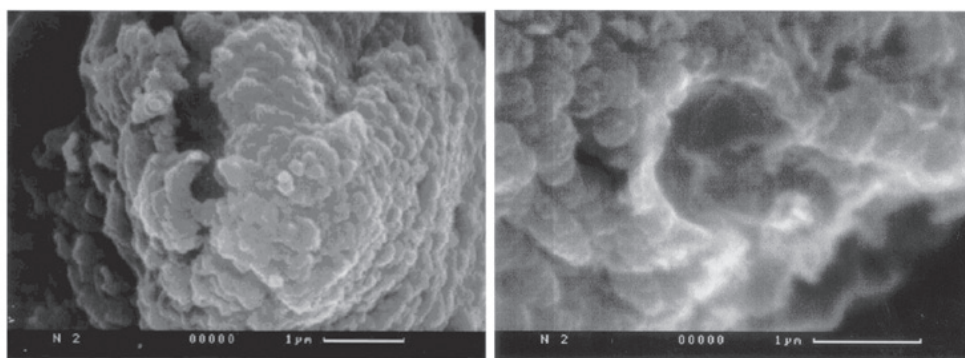


Figure 12. The carbon fibre surface [18].

### 5.3 Low-threshold EE from graphene

There also is a more fundamental issue: in many cases, carbon nanoclusters (nanotubes and graphenes) are present on the carbon surface (Figs 11 and 12). The extremely low excitation threshold of field emission (Section 4) assumes that explosive emission (EE) excited by field emission also has an extremely low threshold. This assumption was completely confirmed in our experiments [8, 23]. It was shown that EE from graphene arrays can be initiated by a voltage as low as  $\leq 10$  kV. The EE current pulse shape reproduced fairly well the shape of the voltage pulse. The current magnitude in a fixed anode–cathode gap varied with voltage, changing from 30 to 120 A.

Characteristic of the EE current pulse is the sharp leading edge with an almost instant “saturation” (Fig. 13). This proves that EE evolution is virtually independent of plasma spread in the vacuum gap. It follows from the latter that the amount of plasma generated during EE from graphene arrays is insignificant, and plasma spread has virtually no effect on the emission process. One would suppose in this case that the current transport in the vacuum gap is entirely governed by the gap macrogeometry and does not depend on the motion of the emission border due to plasma spread according to the Child–Langmuir law, as happens in the case of EE in narrow gaps from metals [5].

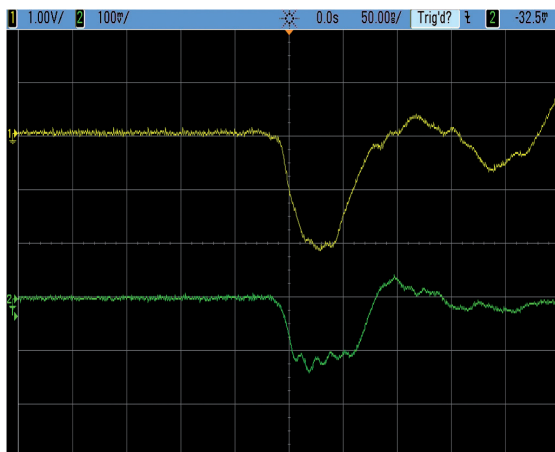


Figure 13. Waveforms of EE voltage and current pulses (upper and lower traces respectively); EE voltage  $U = 25$  kV and EE current  $I = 80$  A; pulse duration is 70 ns.

A direct proof of the above is given by the virtual absence of any noticeable cathode surface erosion. One may infer from the latter that a nanometre size of EE centres yields negligible plasma generation. This is also confirmed by views of the emitting surface by FEM (Fig. 14) and SEM (Fig. 15): the FEM images are virtually unchanged after multiple repeated EE pulses. The same is also apparent from the SEM images (cf. Figs 15a and 15b).

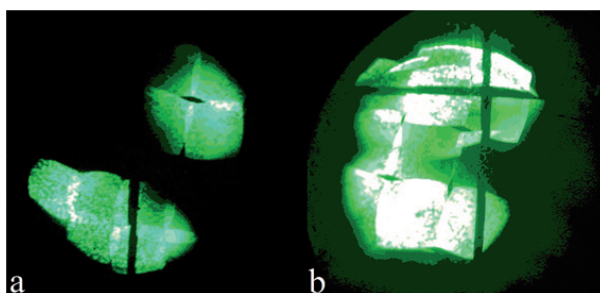


Figure 14. Field emission images: before (a) and after (b) explosive emission.

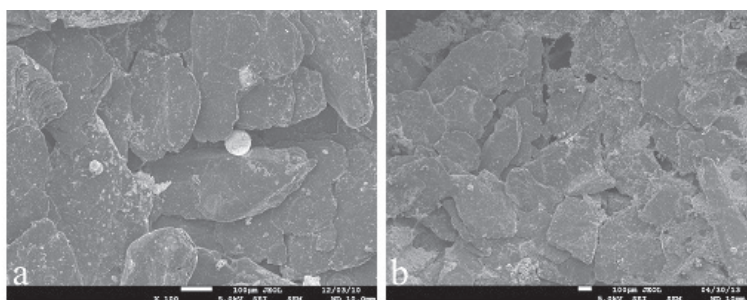


Figure 15. Scanning electron micrographs of the cathode surface: before (a) and after (b) explosive emission.

It is noteworthy that the shape of the current pulse almost copies that of the voltage pulse and remains invariant with time. Such behaviour may be explained by the fact that many field emission centres explode simultaneously. This is because they are uniformly distributed over the emitting surface. For example, Fig. 14 shows that the field emission centres initiating EE are uniformly distributed over the cathode surface. Since they explode almost simultaneously, EE is excited for a short time (see the leading edge of the EE pulse in Fig. 13). Exploding centres have a nanometre size; therefore, the amount of exploding material is insignificant and the moving boundary of the rarefied expanding plasma of EE has a negligible influence on the current in the vacuum diode according to the 3/2 power law for a diode with a moving emission boundary [5].

## 6. Applications

In the last decades, two prospective areas of practical applications have been connected with field emissive processes: vacuum nanoelectronics (VNE) [1 (Ch. 8), 20–22], which uses field emission; and high-power electronics (HPE) [2, 3, 6, 23], based on the EE phenomenon.

### 6.1 Vacuum nanoelectronics

Vacuum nanoelectronics (VNE) is a new field in micro- and nanoelectronics, which has been developed during the recent past few decades. VNE is based on the employment of electrons in vacuum using active elements with dimensions of tenths and hundredths of a micrometre. Practically, a field electron emitter is used as an active element in VNE systems. By employing microscopic anode-to-cathode gaps, one can build devices with a field emission cathode controlled with a potential of tens of volts.

VNE comprises devices and active system components of nanometre size. It presents a sort of alternative to solid state electronics, employing the ballistic motion of electrons in vacuum instead of the transport of current carriers (electrons and holes) in semiconductors.

The small dimensions of a field electron emitter provide an opportunity of bringing the size of the active elements down to a few tens of atomic dimensions (i.e., down to  $10^{-6}$ – $10^{-7}$  cm). Some recent experimental data indicate the existence of active elements of a size around the atomic scale (1–3 Å) made with special materials (e.g., carbon nanotubes [24]).

The small dimensions of field electron emitters also permit achieving a high density of active elements, of up to  $10^8$ – $10^{10}$  cm<sup>-2</sup>, and even up to  $10^{12}$  cm<sup>-2</sup> [24] if one employs such “self-organizing” systems like nanotubes.

### 6.2 The advantages of VNE

The advantages of VNE as compared to solid state electronics are as follows:

1. No dissipation of energy from electron transport in the medium, i.e., *in vacuo*. That gives vacuum microelectronics devices advantages for certain classes of devices, such as those generating high power at high frequencies;
2. VNE devices act at high speed due to the virtual lack of inertia in the field emission process and a very small electron transport time in the vacuum gap, which permits the design of fast-acting high-frequency devices;

3. A marked nonlinearity of the field emission current–voltage characteristics, which permits design of frequency converters and multipliers;
4. No energy expenses—no cost of electron emission due to the quantum origin of the tunnelling process;
5. A high radio tolerance and heat resistance of the emitters.

### **6.3 Main VNE applications**

1. The most outstanding and widespread application is the production of flat low-voltage displays of high brightness and high resolution based on field emission arrays (FEA);
2. Employment of nano-field emission cathodes in electron optics systems of superhigh resolution (in scanning and transmission electron microscopes, in electron lithography systems, Auger electron spectrometers and in tunnel microscopy);
3. Production of active elements for integrated circuits (diodes, transistors etc.);
4. Employment in microwave devices;
5. In devising different types of pressure gauges, magnetic field gauges etc.;
6. In devising new type of ion sources;
7. Realization of new, very efficient production technologies for microelectronics (lithography, etc.).

FE applications particular to VNE are represented in refs 1 (Ch. 8) and 22.

### **6.4 Field emission arrays from carbon nanoclusters**

One of the major problems of modern vacuum nanoelectronics is the fabrication of high efficiency, low voltage field electron emitters with a large working area. The traditional method of fabricating field emitters is based on the use of multineedle field emission cathodes and precision technological processes based on electron lithography techniques. As a cathode material, metals and semiconductors are usually used, which, unfortunately, have rather high work functions (4–5 eV) [20–22].

An alternative development path in vacuum microelectronics is the relatively inexpensive technology of planar field emission cathodes based on films and coatings of various allotropic forms of carbon such as nanoclusters [1, 2, 7, 9, 22]. Carbon nanoclusters and, particularly, nanotubes and graphene can be self-organizing structures that permit, in principle, creation of field emission arrays according to a completely new paradigm.

New vacuum nanoelectronics systems with field cathodes created by means of low-threshold FE made of nanotubes and graphenes are likely to emerge.

### **6.5 High-power electronics**

The possibility to produce high currents has led to the development of a new field of high-current emission electronics based on these processes. Pulsed high-current accelerators of electrons have been designed for currents up to  $10^6$  A. Such accelerators have found application in thermonuclear research for the generation of high-power microwave radiation and for pumping lasers in various technological processes [3, 6, 25, 26].

### 6.6 Nanosecond accelerators

One of the first successful efforts to create powerful nanosecond impulse devices for different applications (defectoscopy, impulse X-ray techniques, ballistics tasks etc.) were engineered and completed under the direction of W.P. Dyke of the Field Emission Corporation (Oregon) [26, 27; see also ref. 6].

It was formerly supposed that these nanosecond electron accelerators used multicusp field emission cathodes but after the discovery of EE it was realized that the source of the powerful electron jets was not field emission but explosive emission.

Powerful nanosecond accelerators of different types functioning on the basis of EE are described in Mesatzs' monographs [see ref. 3].

### 6.7 Portable Roentgen apparatus (PRA)

The first portable Roentgen apparatus (PRA) was proposed by Prof. Tsukerman [28, 29]. It was supposed that the source of the electrons was classical field emission. This misunderstanding of the emission mechanism prevented their exploitation. PRA based on the explosive emission from high-melting point cathodes (W, Ta, Mo), were serially produced in the USSR under the supervision of Prof. N. Komjak. This technique was developed by E. Peliks and others (reviews in refs 30 and 31).

### 6.8 X-ray tubes based on carbon nanoclusters

The explosive electron emission from carbon materials has been successfully employed in developing a new class of portable X-ray devices [31, 32]. The device has been created on the basis of low-threshold explosive electron emission from carbon nanoclusters [32], which allowed the development of universal X-ray tubes working in a wide interval of voltage (15–150 kV) and wavelength. Such equipment has enhanced research possibilities in medicine and biology. A block scheme of the apparatus is shown in Figure 16. Examples of roentgenograms obtained with the help of PRA are shown in Figs 17–19.

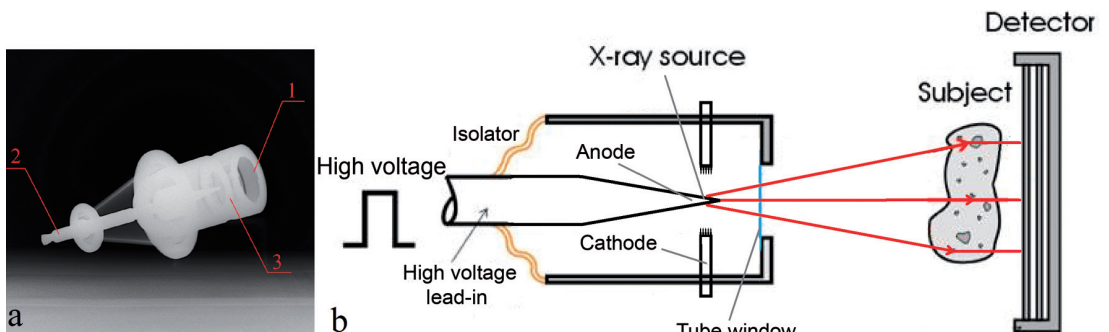


Figure 16. (a) X-ray image of an X-ray tube: (1) output window; (2) anode lead; (3) anticathode; (b) principle of PRA operation.



Figure 17. Picture of a human hand, obtained with a nanosecond pulsed X-ray machine.

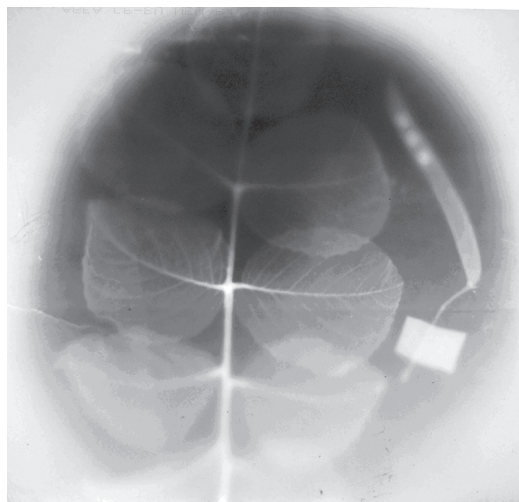


Figure 18. Leaf of a tree.



Figure 19. Inside an attaché case.

Salient characteristics of PRA are noted in Table 4 followed by a list of potential applications of the apparatus.

Table 4. Characteristics of PRA.

Accelerating voltage	15–150 kV
Beam current	50–500 A
X-ray pulse duration	10–20 ns
Repetition rate for short-pulse mode	up to 500 Hz
Spot diameter	1 mm
Total weight (with high-voltage source)	3.5 kg

## Potential applications of portable X-ray devices (PRA)

1. Medicine
2. Defectoscopy (low-Z (atomic number) materials)
3. Biological objects
4. X-ray lithography
5. Criminology
6. Emergency situations
7. Antimicrobe disinfection
8. Rapid baggage checking and screening
9. Security devices
10. Radiation medicine.

**Acknowledgments**

The author tenders heartfelt gratitude to his collaborators and friends. In the first place he thanks Prof. A.V. Kocheryjenkov, Prof. L.A. Shirochin, Dr A.A. Kantonistov and Dr M.A. Polyakov. He also appreciates the technical assistance of V. Pozhinsky, I. Zakirov and D. Fomin. This work was supported by the Russian Foundation for Basic Research, grant no 13-02-01015.

**References**

1. G.N. Fursey. *Field Emission in Vacuum Microelectronics*. New York: Kluwer Academic/Plenum (now Springer) (2005).
2. G.N. Fursey. Field emission in vacuum micro-electronics. *Applied Surface Science* **215** (2003) 113–134.
3. G.A. Mesyats. *Cathode Phenomena in a Vacuum Discharge: the Breakdown, the Spark and the Arc*. Moscow: Nauka (2000).
4. G.N. Fursey and P.N. Vorontsov-Velyaminov. Qualitative model of vacuum arc initiation. *Zh. Tech. Fiz.* **37** (1967) 1870–1888.
5. S.P. Bugaev, A.M. Iskol'ski, G.A. Mesyats and D.I. Proskurovskii. Electron-optical observation of initiation and development of pulse breakdown of short vacuum gap. *Zh. Tech. Fiz.* **37** (1967) 2206–2208.
6. G.N. Fursey. Power electron sources using field emission. In: *Cold Cathodes* (ed. M.I. Elinson), pp. 241–269. Moscow: Sovetskoe Radio (1974).
7. A. Yafyasov, V. Bogevolnov, G. Fursey, B. Pavlov, M. Polyakov and A. Ibragimov. Low-threshold field emission from carbon nano-clusters. *Ultramicroscopy* **111** (2011) 409–414.
8. G.N. Fursey, M.A. Polyakov, A.A. Kantonistov, A.M. Yafyasov, B.S. Pavlov and V.B. Bozhevol'nov. Field and explosive emissions from graphene-like structures. *Technical Phys.* **58** (2013) 845–851.
9. G.N. Fursey, M.A. Polyakov, B.S. Pavlov, A.M. Yafyasov and V.B. Bogevolnov. Exceptionally low threshold of field emission from carbon nanostructures. *Proc. 24th International Vacuum Nanoelectronics Conference (IVNC)*, pp. 3–4. Wuppertal, 18–22 July 2011.
10. R.E. Burgess, Kroemer and J.M. Houston. Corrected values of Fowler–Nordheim field emission function  $\vartheta(y)$  and  $S(y)$ . *Phys. Rev.* **90** (1953) 515.
11. Yu.V. Bozhevolnov and A.M. Yafyasov. Structurization of nanocarbon upon relaxation of chemically activated plasma. In: *Explosive Production of New Materials: Science, Technology, Business and Innovations* (eds A.A. Deribas and Yu.B. Scheck), pp. 20–22. Moscow: Tourus Press (2012).
12. G.N. Fursey, D.V. Novicov, G.A. Dyhzhev, A.V. Kotcheryzhenkov and P.O. Vassiliev. The field emission from carbon nanotubes. *Appl. Surf. Sci.* **215** (2003) 135–140.

13. R.H. Fowler and L. Nordheim. Electron emission in intense electric fields. *Proc. R. Soc. Lond. A* **119** (1928) 173–181.
14. G.N. Fursey, M.A. Polyakov, A. A. Kontonistov, A.M. Yafyasov, B.S. Pavlov and V.B. Bogevolnov. Extremely low threshold of field emission from graphene nanoclusters. *Proc. 25th International Vacuum Nanoelectronics Conference (IVNC 2012)*, pp. 98–99. Jeju, Korea, 9–13 July 2012. <http://toc.proceedings.com/15996webtoc.pdf>
15. R.G. Forbes and J.P. Xanthakis. Field penetration into amorphous-carbon films: consequences for field-induced electron emission. *Surf. Interface Anal.* **39** (2007) 139–145.
16. S.P. Kurdyumov. Evolution and self-organization laws in complex systems. *Int. J. Modern Phys. C* **1** (1990) 299–397.
17. G.N. Fursey, L.A. Shirochin and L.M. Baskin. Field emission processes from liquid-metal surface. *J. Vac. Sci. Technol. B* **15** (1997) 410–421.
18. P. Morgan. *Carbon Fibers and their Composites*. Boca Raton: CRC Press (2005).
19. G.N. Fursey, D.V. Novikov and V.I. Petrick. Low-threshold field electron emission from carbon nanoclusters formed upon cold destruction of graphite. *J. Tech. Phys.* **54** (2009) 1048–1051.
20. I. Brodie and C.A. Spindt. Vacuum microelectronics. In: *Advances in Electronics and Electron Physics*, vol. 83, pp. 1–106. New York: Academic Press (1992).
21. I. Brodie and P.R. Schwoebel. Vacuum microelectronic devices. *Proc. IEEE* **82** (1994) 1006–1034 .
22. A.V. Eletskii. Carbon nanotubes and their emission properties. *Phys. Usp.* **45** (2002) 369–402.
23. G. Fursey, M. Polyakov and V. Bogevolnov. Experimental study of the electron field emission and an explosive field emission from graphene and graphene-like structures. *Proc. 26th International Vacuum Nanoelectronics Conference (IVNC 2013)*, 8–12 July 2013, Roanoke, Virginia, USA.
24. N.I. Sinitsyn, G.V. Torgashov, Yu.V. Gulyaev, S.A. Knyazev, Z.I. Buyanova, A.I. Zhbanov, O.E. Glukhova, I.G. Torgashov, S.L. Ryabushkin and V.I. Elmanov. Electron field emission from nanocluster carbon-metal films. *Technical Digest of 12th International Vacuum Microelectronics Conference*, pp. 252–254. Darmstadt (1999).
25. W.P. Dyke and W.W. Dolan. Field emission. In: *Advances in Electronics*, vol. 8, pp. 88–155. New York: Academic Press (1956).
26. W.P. Dyke and F.M. Charbonnier. Field emission technology. In: *Advances in Electron Tube Techniques* (ed. D. Slater), pp. 199–209. Oxford: Pergamon Press (1963).
27. F.J. Grundhauser, W.P. Dyke and S.D. Bennett. A 50 millimicrosecond flash X-ray photography system for hypervelocity research. *5th International Congress on High Speed Photography*, 18 October 1960. Washington D.C.: Field Emission Corporation (1960).
28. V.A. Tsukerman, L.V. Tarasova and S.I. Lobov. New sources of X-rays. *Sov. Phys. Usp.* **14** (1971) 61–71.
29. V.A. Tsukerman. Portable X-ray sources. *Vestn. Akad. Nauk SSSR* **41** (1971) 18–25 (in Russian).
30. G.N. Fursey, E.A. Pelix. The new generation of medical X-ray discrete instrumentation. *Practical High-Power Electronics* **44** (2011) 47–51 (in Russian).
31. E.A. Pelix. X-ray pulse apparatus based on explosive electron emission. *Proc. 17th World Conference on Nondestructive Testing*, 25–28 October 2008, Shanghai. <http://www.ndt.net/article/wcndt2008/papers/7.pdf>
32. G.N. Fursey (Fursey), L.A. Shirochin and P.N. Bepalov. *X-ray Tube*. Russian Federation Patent No 2308781 (20 October 2007), Bulletin 29.

